Molecular Crystals and Liquid Crystals

Publication details, including instructions for authors and subscription information:
http://www.tandfonline.com/loi/gmcl20

The Improvement of Surface Energy of BPDA-EDA Polyimide by Controlling Molecular-Level Structure

Kyung-Hoe Kim [a], Yong-Gwon Kim [b] & Younghwan Kwon [a]

[a] Department of Chemical Engineering, Daegu University, Kyungbuk, Korea

[b] Korean Fire Protection Association, Youngdeungpo, Seoul, Korea

Version of record first published: 10 Nov 2009

To cite this article: Kyung-Hoe Kim, Yong-Gwon Kim & Younghwan Kwon (2009): The Improvement of Surface Energy of BPDA-EDA Polyimide by Controlling Molecular-Level Structure, Molecular Crystals and Liquid Crystals, 513:1, 60-78

To link to this article: http://dx.doi.org/10.1080/15421400903192848

Mol. Cryst. Liq. Cryst., Vol. 513, pp. 60–78, 2009

ISSN: 1542-1406 print/1563-5287 online
DOI: 10.1080/15421400903192848

Taylor & Francis
Taylor & Francis Group

The Improvement of Surface Energy of BPDA-EDA Polyimide by Controlling Molecular-Level Structure

Kyung-Hoe Kim[1], Yong-Gwon Kim[2], and Younghwan Kwon[1]
[1]Department of Chemical Engineering, Daegu University, Kyungbuk, Korea
[2]Korean Fire Protection Association, Youngdeungpo, Seoul, Korea

The surface properties (water sorption and repellency, adhesion) are closely related to the surface tension of polymer solid. Critical surface tension γ_C and surface tension γ_S of a polymer solid have been estimated by the contact angle method by our quantitative imaging system. BPDA (3,3′,4,4′-biphenyl tetracarboxylic dianhydride) – EDA (4,4′-ethylenedianiline) polyimide was successfully synthesized. The critical surface tensions γ_C were analyzed by a Zisman plot, a Young-Dupré-Good-Girifalco plot, and a log $(1+\cos\theta)$ vs log γ_L plot. The surface tension γ_S of BPDA-EDA polyimide was evaluated using the geometric mean equation and our multiple regression analysis. The calculated values of γ_S^d (a dispersion component), γ_S^p (a polar component), γ_S^h (a hydrogen bonding component), and γ_S are 30.49, 4.52, 0.08, and 35.09 $mN \cdot m^{-1}$, respectively. The γ_S of BPDA-EDA polyimide containing two methylene groups is smaller than those of the polyimides containing both methylene group and ether group.

Keywords: contact angle; critical surface tension; imaging method; polyimide; solid surface energy

INTRODUCTION

Polyimides have been used in a wide variety of microelectronic applications that include interlayer dielectrics in integrated circuits [1], inter-metal insulators in high density interconnect packaging schemes [2], and thermo-mechanical passivation buffer protection layers. They are thermally stable polymers that exhibit excellent chemical resistance, good mechanical properties, and superior dielectric properties [3–5]. However, polyimide films are known to absorb water

Address correspondence to Prof. Kyung-Hoe Kim, Department of Chemical Engineering, Daegu University, Kyungbuk, 712-714, Korea (ROK). E-mail: khk9509@daegu.ac.kr

in some amounts [6–9], despite their relatively high chemical resistance characteristics [10,11]. Water absorbed in polyimide films causes metal corrosion, package cracking, delaminating, failures of the adhesion to metal, and degradation of dielectric properties [12–15]. To predict the behavior of polyimides and to optimize their fabrication, it is important to understand the relationship between polyimides structure and their surface properties [16–19]. The surface properties (water sorption and repellency, adhesion) are closely related to the surface tension of polymeric solid. Estimation of surface tension of polymer solid has generally been made by the contact angle method.

The existed experimental techniques for measuring a contact angle are as follows. Several investigators [20,21] simply viewed a sessile drop through a comparator microscope fitted with a goniometer scale, thus measuring the angle directly. Ottewill made use of a captive bubble method [22] wherein a bubble formed by manipulation of a micrometer syringe was made to contact the solid surface. The contact angle might be measured from photographs of the bubble profile, or directly, by means of a goniometer telemicroscope [23]. A reflected light method [24] was engaged in measuring the contact angle. The above-mentioned methods are inaccurate and irreproducible because a testing drop for contact angle measurement can be easily evaporated due to its tiny size and volatility. However, our lab-made quantitative imaging system could provide accurate and reproducible value of a contact angle since the computing system instantly grab the contact angle image and then store it to analyze.

BPDA-EDA polyimide was newly synthesized to investigate the effect of the introduced methylene group on the surface property. A contact angle was measured by a quantitative imaging system to investigate the relationship between a newly synthesized polyimide and its surface property. Three different groups of testing liquids [25], e.g., dispersion, polar, hydrogen bonding liquids were used to measure the contact angle θ on a BPDA-EDA polyimide film. Critical surface tensions γ_C were evaluated by a Zisman plot, a Young-Dupré-Good-Girifalco plot, and a log $(1+\cos\theta)$ vs log (γ_L) plot [26]. The surface tension γ_S of BPDA-EDA polyimide was determined by a geometric mean equation and the multiple regression analysis.

1. THEORETICAL BACKGROUND

1.1. Young's Equation

The equilibrium contact angle (abbreviated θ here) for a liquid drop on a solid surface is usually discussed in terms of Young's equation;

$$\gamma_L \cos\theta = \gamma_S - \gamma_{SL} \tag{1}$$

1.2. Critical Surface Tension

1.2.1. *Zisman Plot*

The concept of critical surface tension was first proposed by Fox and Zisman [20,27,28]. An empirical rectilinear relation was found between $\cos\theta$ and γ_L for a series of testing liquids on a given solid. When homologous liquids are used, a straight line is often obtained. When nonhomologous liquids are used, however, the data are often scattered within a rectilinear band or give a curved line. The intercept of the line at $\cos\theta = 1$ is the critical surface tension γ_C [29]. The $\cos\theta$ vs γ_L is known as the Zisman plot.

1.2.2. *Young-Dupré-Good-Girifalco Plot*

Fowkes [30], Good [31,32], Good and Girifalco [33] introduced an interaction parameter Φ_G, defined by.

$$\Phi_G = W_a/(W_{c1}W_{c2})^{0.5} \tag{2}$$

They presented the following equation

$$W_a = 2\Phi_G/(\gamma_S\gamma_L)^{0.5} \tag{3}$$

Using Eq. (1) and Young-Dupré's equation

$$W_a = \gamma_L(1 + \cos\theta) \tag{4}$$

Equation (5) can be derived and determine the magnitude of the interfacial tension, γ_{SL}.

$$W_a = \gamma_S + \gamma_L - \gamma_{SL} \tag{5}$$

W_a and γ_{SL} are very important parameters for wettability and adhesion.

Combining Eq. (3) with Eq. (4) leads to the equation of Young-Dupré-Good-Girifalco:

$$1 + \cos\theta = 2\Phi_G(\gamma_S/\gamma_L)^{0.5} \tag{6}$$

The Young-Dupré-Good-Girifalco plot expressed by the $(1 + \cos\theta)$ vs $\gamma_L^{-0.5}$ gives rise to a good straight line with the experimental data obtained by the contact angle θ of homologous liquids on a polymer solid. However, in many cases the straight line greatly deviated from

the origin with the polarity of liquids [34]. In such cases, the straight line can be expressed as:

$$1 + \cos\theta = \lambda\gamma_{\mathrm{L}}^{-0.5} + \phi \tag{7}$$

where λ and ϕ are the slope and the intercept of $(1+\cos\theta)$ at $\gamma_{\mathrm{L}}^{-0.5}=0$ in the $(1+\cos\theta)$ vs $\gamma_{\mathrm{L}}^{-0.5}$ plot known as the Young-Dupré-Good-Girifalco plot. These parameters are constant with homologous liquids. The critical surface tension γ_{C} can be obtained from the value of γ_{L} at $\theta \to 0$.

Using Eq. (7), Young-Dupré's equation (4) and Good-Girifalco's equation (3), and neglecting equilibrium spreading pressure, the Good-Girifalco interaction parameter Φ_{G} is expressed as:

$$\Phi_{\mathrm{G}} = (1/2\gamma_{\mathrm{S}}^{0.5})\left[(2-\phi)\gamma_{\mathrm{C}}^{0.5} + \phi\gamma_{\mathrm{L}}^{0.5}\right] \tag{8}$$

The parameter Φ_{G}^{0}, defined as Φ_{G} at $\theta \to 0$, is expressed as follows.

$$\Phi_{\mathrm{G}}^{0} = (\gamma_{\mathrm{C}}/\gamma_{\mathrm{S}})^{0.5} \tag{9}$$

1.2.3. *The Log (1+ cos θ) versus Log (γ_L) Plot*

As the interaction between liquid and solid is approximated by the use of the geometric mean law, Φ_0 is defined as the indication of polarity in Φ_{G}. Furthermore, we also took account of an adjustable parameter X_{LS} within Φ_{G} as a deviation from the interaction estimated by the geometric law [34]. Thus Φ_{G} is represented by:

$$\begin{aligned}\Phi_{\mathrm{G}} &= (X_{\mathrm{L}}^{\mathrm{d}}X_{\mathrm{S}}^{\mathrm{d}})^{0.5} + (X_{\mathrm{L}}^{\mathrm{p}}X_{\mathrm{S}}^{\mathrm{p}})^{0.5} + X_{\mathrm{LS}} \\ &= \Phi_0 + X_{\mathrm{LS}}\end{aligned} \tag{10}$$

Wu [35] reported that the polarity $X_{\mathrm{j}}^{\mathrm{p}}$ was estimated with the solubility parameter δ and the polarity component of the solubility parameter δ^{p} by the following equation:

$$X_{\mathrm{S}}^{\mathrm{p}} = (\delta^{\mathrm{p}}/\delta)^2 \tag{11}$$

Also, the parameter a, determined with the polarity and X_{LS}, is introduced into Φ_G as follows:

$$\begin{aligned}&\Phi_{\mathrm{G}} = \Phi_0(\gamma_{\mathrm{L}}/\gamma_{\mathrm{S}})^{a} \\ &a = \left[\log\left(1+\frac{X_{\mathrm{LS}}}{\Phi_0}\right)\right] \Big/ \log(\gamma_{\mathrm{L}}/\gamma_{\mathrm{S}}) \\ &a < 0.5 \quad \text{for } \mathrm{d}\cos\theta/\mathrm{d}\gamma_{\mathrm{L}} < 0\end{aligned} \tag{12}$$

The Φ_0 is equal to the bonding efficiency parameter of Kaelble and Uy [36]. Therefore, Φ_G^0 is expressed by:

$$\Phi_G^0 = \left[(X_C^d X_S^d)^{0.5} + (X_C^p X_S^p)^{0.5}\right](\gamma_C/\gamma_S)^a \tag{13}$$

where X_C^d is the ratio of γ_C obtained with dispersion liquids and γ_C obtained with polar or hydrogen bonding liquids [34]. By solving Eqs. (9) and (13), solid surface tension γ_S can be calculted from Eq. (14):

$$\gamma_S = \gamma_C[(X_C^d X_S^d)^{0.5} + (X_C^p X_S^p)]^{2/(2a-1)} \tag{14}$$

Also, the reversible work of adhesion W_a is expressed by:

$$W_a = 2\Phi_0(\gamma_S^{0.5-a}\gamma_L^{0.5+a}) \tag{15}$$

Consequently, combining Eq. (15) with Young-Dupré's equation (4) leads to:

$$\log(1+\cos\theta) = -\Psi\log(\gamma_L) + \log(2\Phi_0\gamma_S^{0.5-a}) \tag{16}$$

Using Eq. (16), the parameter a is determined with the slope $\Psi = (0.5 - a)$ from log $(1 + \cos\theta)$ vs log (γ_L) plot and γ_C can be found by extrapolating the linear function to $\log(1+\cos\theta) = \log 2$.

1.3. Surface Tension of Polymer Solid

Kitazaki and Hata [25] extended Fowkes' equation [30] to the following equation.

$$\gamma_S = \gamma_S^d + \gamma_S^p + \gamma_S^h \tag{17a}$$

$$\gamma_L = \gamma_L^d + \gamma_L^p + \gamma_L^h \tag{17b}$$

They proposed that the surface tension of polymer film γ_S can be considered as a sum of a dispersion component γ_S^d, a polar component γ_S^p and a hydrogen bonding component γ_S^h. Liquid surface tension γ_L is also expressed as a sum of a dispersion component γ_L^d, a polar component γ_L^p, and a hydrogen bonding component γ_L^h. Using the work of adhesion W_a, the extended Fowkes' Eq. (17) is expressed in the following equation.

$$W_a = 2[(\gamma_L^d\gamma_S^d)^{0.5} + (\gamma_L^p\gamma_L^p)^{0.5} + (\gamma_L^h\gamma_S^h)^{0.5}] \tag{18}$$

By solving the Young-Dupré Eqs. (4) and (18), geometric mean Eq. (19) is obtained.

$$\gamma_L(1+\cos\theta) = 2[(\gamma_L^d\gamma_S^d)^{0.5} + (\gamma_L^p\gamma_L^p)^{0.5} + (\gamma_L^h\gamma_S^h)^{0.5}] \tag{19}$$

Equation (19) can be transformed in Eq. (20)

$$z = (\gamma_S^d)^{1/2} + (\gamma_S^p)^{1/2}\, x + (\gamma_S^h)^{1/2} y \tag{20}$$

where

$$x = \sqrt{\frac{\gamma_L^p}{\gamma_L^d}}, \quad y = \sqrt{\frac{\gamma_L^h}{\gamma_L^d}}, \quad z = \frac{\gamma_L(1+\cos\theta)}{2(\gamma_L^d)^{0.5}}$$

The surface tension of polymer solid γ_S and its fractional components $(\gamma_S^d, \gamma_S^p, \gamma_S^h)$ can be determined by contact angles measured by three different group of test liquids [25] and Eq. (20).

2. EXPERIMENTAL

2.1. Synthesis of BPDA-EDA Polyimide

It was investigated how surface properties were affected by introducing both methylene groups and ether group to the main chain of newly synthesized polyimide. Polyimide is an imide group-containing polymer synthesized by condensation polymerization of dianhydride with diamine. Depending on the structure of the chemical radicals attached to the imide group, polyimide can be aliphatic or aromatic, linear or branched.

This study polymerized BPDA (3,3′,4,4′-biphenyltetracarboxylic dianhydride; Chriskev Co., Inc.) with lab-synthesized EDA (4,4′-ethylenedianiline). The preparation process of polyamic acid and polyimide of BPDA-EDA demonstrated in Figure 1. A diamine of EDA and a solvent of NMP (*N*-methyl-2-pyrrolidone, Aldrich Chem. Co., Inc.) were introduced into a four-necked flask (500 ml) equipped with a thermocouple, a stirrer, and a nitrogen inlet. The mixtures were stirred thoroughly in a nitrogen environment. After dissolving EDA completely, BPDA was put into the flask at 1:1 stoichiometric ratio. A solvent soluble polyamic acid precusor was formed by the slow reaction of reaction mixtures for 5 h. The solid content of viscous reaction mixtures was about 15% (w/v) by NMP solvent.

A spin coater (Model 301 series, Able Co.) was used to make a thin film from the polyamic acid of BPDA-EDA by coating on silicone wafer.

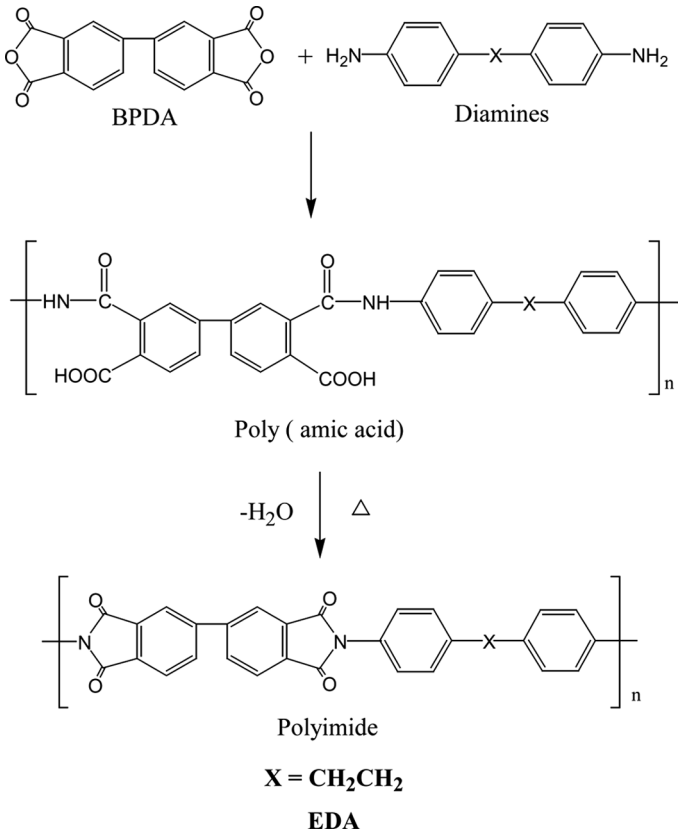

FIGURE 1 Synthetic process of BPDA-EDA polyimide.

After prebaking the coated film in an 80°C vacuum oven for an hour, an additional process was performed by curing it in 150°C for 30 min, 250°C for 30 min, 350°C for 1 h at 10°C/min of heating rate under nitrogen. A distilled water bath was employed to separate the coated polyimide film from silicone wafer. The separated film was used for contact angle measurement after complete drying in the oven.

2.2. IR Spectroscopy

FT-IR Spectrometer (Genesis II, Mattson Instrument) was used to confirm if a BPDA-EDA polyimide was successfully synthesized. Examining the absorption bands of the carbonyl group (C=O) and the imide ring (C−N) could provide the right information of the imidization reaction.

2.3. Contact Angle Measurement by Quantitative Imaging System

A CCD camera (Model WV-BL 600, Panasonic) was connected to a zoom microscope (Model A52953, Edmund Scientific Ltd.) for acquiring contact angle images by a computer system. A personal computing system saved contact angle images captured by a Frame grabber (Model DT2867, Data Translation Inc.), the CCD camera, and the zoom microscope. The frame grabber possesses 256 gray scale photography and the resolution of 640×480 pixels. The captured contact angle image was quantitatively analyzed by an imaging software (Global Lab® Image, Data Translation Inc.) and a separate multisync monitor (Syncmaster 1000p, Samsung Co.).

Figure 2 indicates a schematic diagram of the quantitative imaging system. The value of contact angle was determined by the following experimental procedure and imaging analysis method. A microsyringe injected an 1 mm size of a testing liquid to neglect the gravity effect. As soon as a testing liquid in Table 1 was equilibrated, a contact angle image was instantly grabbed. An 1-mm-diameter stainless ball was engaged to calibrate the actual dimension of the enlarged image of the contact angle. Image enhancement was performed to differentiate solid film from the sessile drop and the background from the sessile drop. After determining the radius r of the baseline formed by the solid film and the sessile drop, the height h of the sessile drop was

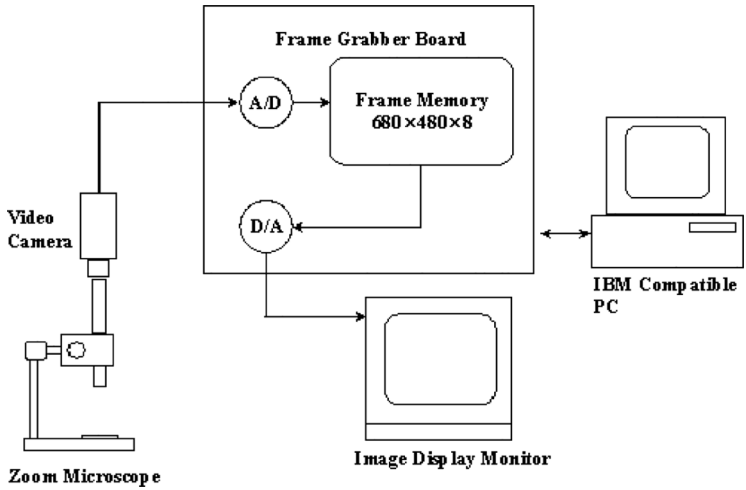

FIGURE 2 Schematic diagram of the image processing system.

TABLE 1 The Contact Angle θ on BPDA-EDA Polyimde Film and Surface Tensions of All Testing Liquids at 20°C [mN·m^{-1}]

Species	Liquid	Contact angle θ (°)	γ_L^d	γ_L^p	γ_L^h	γ_L	X_L^p
Dispersion solution	Octane	Spreading	21.8	0	0	21.8	0
	Nonane	Spreading	22.9	0	0	22.9	0
	Decane	Spreading	23.9	0	0	23.9	0
	Undecane	Spreading	24.7	0	0	24.7	0
	Tetradecane	Spreading	26.7	0	0	26.7	0
	Hexadecane	Spreading	27.6	0	0	27.6	0
Polar solution	Hexachlorobutadiene	23.7	35.8	0.2	0	36.0	0.006
	1,2-Dibromoethane	34.6	–	–	–	38.9	–
	α-Bromonaphthalene	38.5	44.4	0.2	0	44.6	0.004
	Tetrabromoethane	50.9	44.3	3.2	0	47.5	0.067
Hydrogen solution	Dipropyleneglycol	41.6	29.4	0	4.5	33.9	0.133
	1,3-Butanediol	57.3	–	–	–	37.8	–
	Polyethyleneglycol	69.2	29.9	0.1	13.5	43.5	0.313
	Diethyleneglycol	67.1	31.7	0	12.7	44.4	0.286
	Ethyleneglycol	70.6	30.1	0	17.8	47.7	0.373
	Water	92.7	29.1	1.3	42.4	72.8	0.600

calculated. Since direct reading of the contact angle provided a large experimental error, the contact angle was estimated by the $\theta/2$ method which gave accurate and reproducible results [37,38].

3. RESULTS AND DISCUSSION

3.1. FT-IR Spectra

It is confirmed from Figure 3 that the BPDA-EDA polyimide is successfully synthesized [39]. The strongest absorption occurs at 1720 cm^{-1} (C=O symmetrical stretching). The more useful bands of imide groups are 1780 cm^{-1} (C=O asymmetrical stretching), 1380 cm^{-1} (C−N stretching), 725 cm^{-1} (C=O bending).

3.2. Contact Angles

Before measuring the contact angles formed by water on the BPDA-EDA polymide film, a PTFE (polytetrafluoroethylene) film was used to calibrate the quantitative imaging system and its analysis method. The contact angle on the PTFE film is 108 degree, which is corroborated the value in the literature [40–42]. It is verified that

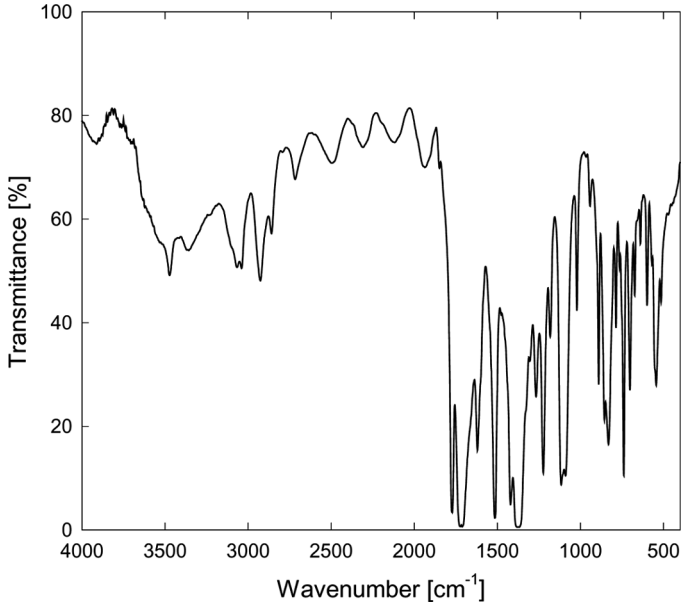

FIGURE 3 FT-IR spectrum of BPDA-EDA polyimide film.

the quantitative imaging system and its analysis method can provide accurate and reproducible values of the contact angle. Contact angles were measured by dispersion, polar, and hydrogen bonding liquids in Table 1. Figure 4 is a typical contact angle image of a liquid drop of ethyleneglycol equilibrated on the BPDA-EDA polyimide film. It can be seen from Table 1 that the values of the contact angle increases with increasing of the surface tensions of the testing liquids used. The largest contact angle was measured by water whose surface tension is the largest among hydrogen bonding liquids. On the other hand, the smallest contact angle was observed by hexa-chlorobutadiene whose surface tension is the samllest among polar liquids. For a group of dispersion testing liquids, however, contact angles are not observed due to their complete spreading on polyimde film.

3.3. Critical Surface Tensions

The Zisman plots for the BPDA-EDA polymide film are shown in Figure 5. Table 2 displays the critical surface tensions estimated by Figure 5. The values of the critical surface tensions by polar and hydrogen bonding liquids are 31.03 and 11.57 $mN \cdot m^{-1}$, respectively.

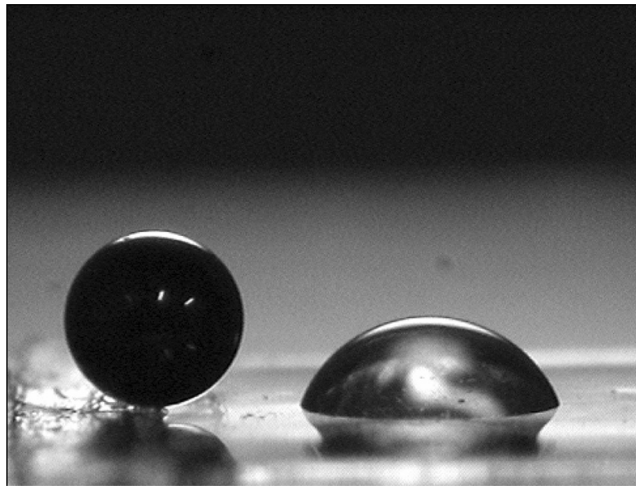

FIGURE 4 Typical contact angle image of a testing liquid drop of ethyleneglycol on BPDA-EDA polyimide film.

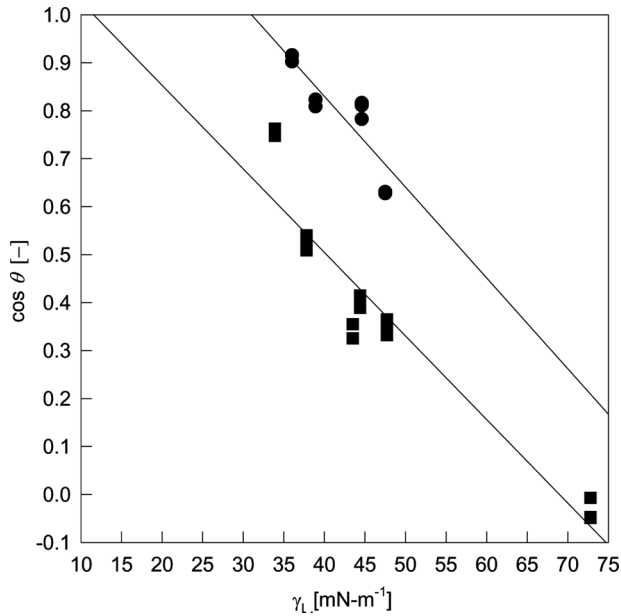

FIGURE 5 Zisman plots for BPDA-EDA polyimide film: ●, Polar liquids; ■, Hydrogen bonding liquids.

TABLE 2 The Critical Surface Tensions γ_C of BPDA-EDA Polyimide Film and the Constants Determined from the $(1+\cos\theta)$ vs $\gamma_L^{-0.5}$ Plot

Polyimide	Plot	Testing liquids	γ_C	ϕ
BPDA-EDA	$\cos\theta$ vs γ_L	Polar	31.03	
		Hydrogen	11.57	
	$(1+\cos\theta)$ vs $\gamma_L^{-0.5}$	Polar	32.32	0.255
		Hydrogen	26.20	−0.614
	$\log(1+\cos\theta)$ vs $\log(\gamma_L)$	Polar	32.41	
		Hydrogen	26.99	

The critical surface tensions by dispersion liquids can not be obtained because of their complete spreading on the polyimide film. The magnitude of critical surface tension, therefore, increases in the following order: hydrogen liquids < polar liquids. When plotting $\cos\theta$ as a function of the polarity of different liquids, different values of critical surface tensions γ_C are obtained. The γ_C for polar liquids is 2.68 times larger than γ_C for hydrogen bonding liquids. The larger variation is illustrated as follows.

On the Zisman plots, empirical relation between $\cos\theta$ and γ_L displays a reasonably straight line when the value of γ_L is in the vicinity of γ_C (in the case of polar liquids). On the other hand, data fitting displays a downwardly convex because a liquid with γ_L much greater than γ_C generally possesses hydrogen bonding [35]. The Zisman plots and the critical surface tensions are corroborated by using the intercept ϕ of $(1+\cos\theta)$ at $\gamma_L^{-0.5}=0$ from the $(1+\cos\theta)$ vs $\gamma_L^{-0.5}$ plot. From Eqs. (6) and (8), the relationship between $\cos\theta$ and γ_L can be rewritten by the following equation.

$$\cos\theta = (2-\phi)(\gamma_C/\gamma_L)^{0.5} + (\phi - 1) \tag{21}$$

Therefore, Eq. (21) indicates a downwardly convex curve. The γ_C values extrapolated by the Zisman plot and estimated by Eq. (21) are provided as γ_c^E (experimental γ_C) and γ_c^T (theoretical γ_C), respectively. Combining Eq. (21) with the ϕ and γ_C values in Table 2 becomes:

$$\text{for Polar liquid:} \quad \cos\theta = 9.92(\gamma_L^{-0.5}) - 0.745$$

$$\text{for Hydrogen bonding liqud:} \quad \cos\theta = 13.381(\gamma_L^{-0.5}) - 1.614$$

Both of the curves fitted by Eq. (21) and the straight dashed line on the Zisman plot by using the least squares method are shown in Figure 6. Better consistency is observed between experimental data and the

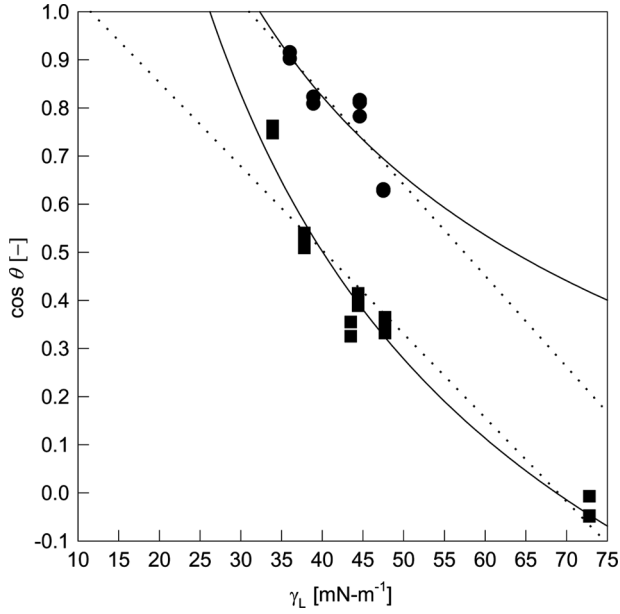

FIGURE 6 Theoretical curves of $\cos\theta$ vs γ_L based on Eq. (21) for BPDA-EDA polyimide film: ●, Polar liquids; ■, Hydrogen bonding liquids; ----- Straight line on the Zisman plots.

theoretical curve estimated by Eq. (21). For the polar liquids, γ_c^E is nearly equal to γ_c^T. On the other hand, γ_c^E is obviously smaller than γ_c^T for the hydrogen bonding liquids. Consequently, it is concluded that the Zisman plot is essentially a downwardly convex curve with polar and hydrogen bonding liquids having $\gamma_C \ll \gamma_L$. This result is consistent with that of Gutowski [43].

Young-Dupré-Good-Girifalco plots represented by the $(1+\cos\theta)$ vs $\gamma_L^{-0.5}$ are shown in Figure 7. The straight lines on the $(1+\cos\theta)$ vs $\gamma_L^{-0.5}$ fitted by the least squares method greatly deviated from the origin. Table 2 indicates that the values of critical surface tensions by polar and hydrogen bonding liquids are 32.32 and 26.20 $mN \cdot m^{-1}$, respectively. From the $(1+\cos\theta)$ vs $\gamma_L^{-0.5}$ polt, γ_C by dispersion liquids also cannot be obtained due to their complete spreading. The magnitude of critical surface tension also increases in the same trend: hydrogen liquids < polar liquids. The values of γ_C estimated with the $(1+\cos\theta)$ vs $\gamma_L^{-0.5}$ polt also have different numbers with varying polarity of liquids used.

The log $(1+\cos\theta)$ vs log γ_L plots are shown in Figure 8. Experimental data are fitted well with the straight lines fitted by the least

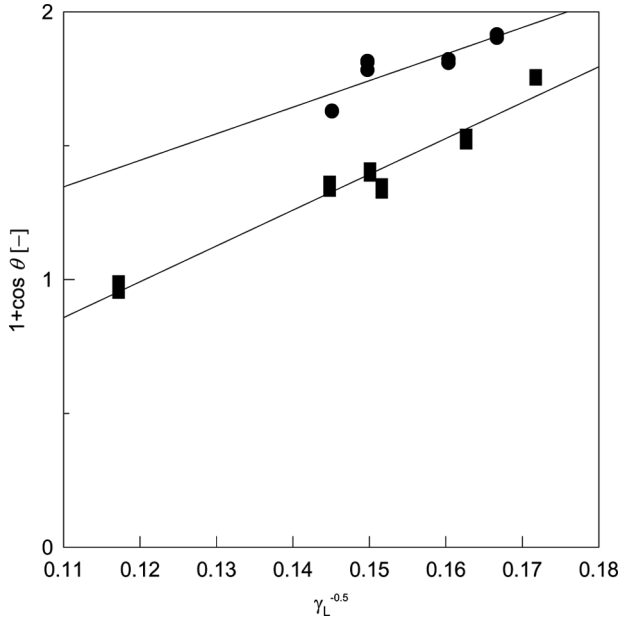

FIGURE 7 Young-Dupré-Good-Girifalco plots for BPDA-EDA polyimide film: ●, Polar liquids; ■, Hydrogen bonding liquids.

squares method. Table 2 indicates that the values of critical surface tensions by polar and hydrogen bonding liquids are 32.41 and 26.99 $\mathrm{mN \cdot m^{-1}}$, respectively. The order of the magnitude of γ_C evaluated with this plot is similar to those on other plots as mentioned before. The γ_C values calculated from the log $(1 + \cos\theta)$ vs log γ_L plot also have different numbers with varying polarity of liquids. The γ_C values by the Zisman plot are smaller than those estimated by either the Young-Dupré-Good-Girifalco plot or the log $(1 + \cos\theta)$ vs log γ_L plot.

3.4. Solid Surface Tension

Figure 9 represents the best correlation of experimental data using a multiple regression analysis [44,45]. The surface tension γ_S of the BPDA-EDA polyimide can be determined by combining contact angles and three known components $(\gamma_L^d, \gamma_L^p, \gamma_L^h)$ with geometric mean Eq. (20). The calculated values of γ_S^d, γ_S^p, γ_S^h, and γ_S are 30.49, 4.52, 0.08, and 35.09 $\mathrm{mN \cdot m^{-1}}$, respectively. Two different Kapton® H films [46] are as follows. The first one is Poly(1,3,5,7-tetraoxo-2,3,6,7-tetrahydro-1H,

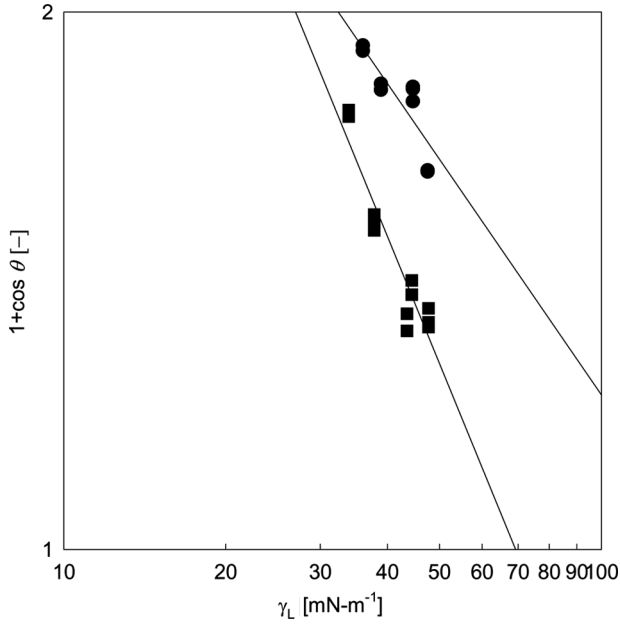

FIGURE 8 $\mathrm{Log}(1+\cos\theta)$ vs $\log\gamma_L$ plots for BPDA-EDA polyimide film: •, Polar liquids; ■, Hydrogen bonding liquids.

5H-benzo[1,2-c:4,5-c′]dipyrrol-2,6-diyl-1,4-phenyleneoxy-1,4-phenylene) whose surface tension γ_S is $37.7\,mN\cdot m^{-1}$ and the polarity is 0.223. The second one is Poly(iminocarbonyl-(4,6-dicarboxy-1,3-phenylene)-carbonylimino-1,4-phenyleneoxy-1,4-phenylene) whose surface tension γ_S is $41.1\,mN\cdot m^{-1}$ and polarity is 0.358. The γ_S of BPDA-EDA polyimide is $35.09\,mN\cdot m^{-1}$ which is 0.85 and 0.93 times smaller than those of Kapton® H films, respectively. The polarity of BPDA-EDA polyimide is 0.131 whose value was located between 0.37 and 0.56 magnitudes of Kapton® H films' polarity, respectively.

The value of γ_S^d is larger than γ_L^d of dispersion liquids (21.8–$27.6\,mN\cdot m^{-1}$). It can be seen from Table 2 that contact angles are not observed because dispersion liquids completely spread on the polyimde film. The reason of complete spreading is that γ_S^d is larger than γ_L^d. It is not because of both the relation of $\gamma_S > \gamma_L$ and polar properties. The γ_C values in Table 2 are generally smaller than γ_S. The two results are well corroborated with those reported by Kiatazaki and Hata [22]. The γ_S of BPDA-EDA polyimide containing two methylene groups is smaller than those of the polyimides containing both methylene group and ether group.

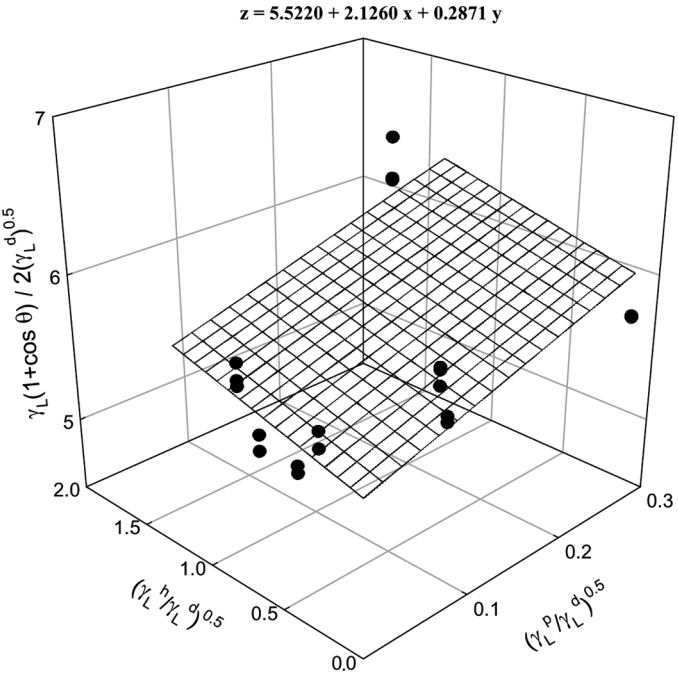

FIGURE 9 Determination of the dispersion (γ_S^d), the polar (γ_S^p), and the hydrogen bonding (γ_S^h) component of the surface tension of BPDA-EDA polyimide by using geometric mean Eq. (20).

4. CONCLUSIONS

It is confirmed that the BPDA-EDA polyimide is successfully synthesized. Contact angles on BPDA-EDA polyimide film were measured by dispersion, polar, and hydrogen bonding liquids. It can be seen that the values of the contact angle increases with increasing of the surface tension of testing liquids used. For a group of dispersion testing liquids, however, contact angles are not observed due to their complete spreading on the polyimide film. The reason can be illustrated by the relation of $\gamma_S^d > \gamma_L^d$.

The γ_C values by the Zisman plot are smaller than those estimated by either the Young-Dupré-Good-Girifalco plot or the log $(1 + \cos\theta)$ vs log γ_L plot. The Zisman plot is essentially a downwardly convex curve with the polar and hydrogen bonding liquids having $\gamma_C < \gamma_L$. Critical surface tensions γ_C calculated from all plots have different values with depending on polarity of liquids. The order of the magnitude of γ_C evaluated with all plots is as follows: hydrogen liquids < polar liquids.

The calculated values of γ_S^d, γ_S^p, γ_S^h, and γ_S are 30.49, 4.52, 0.08 and 35.09 $mN \cdot m^{-1}$, respectively. The γ_S of BPDA-EDA polyimide is 35.09 $mN \cdot m^{-1}$ which is 0.85 and 0.93 times smaller than those of Kapton® H films, respectively. The polarity of BPDA-EDA polyimide is 0.131 whose value was located between 0.37 and 0.56 magnitudes of Kapton® H films' polarity, respectively. The γ_S of BPDA-EDA polyimide containing two methylene groups is smaller than those of the polyimides containing both methylene group and ether group.

NOMENCLATURE

a	parameter defined in Eq. (12) [—]
h	height of the sessile drop [m]
r	radius of the sessile drop [m]
W_a	work of adhesion [J]
W_c	work of cohesion [J]
X_C^d	ratio of γ_C obtained with dispersion liquid [—]
X_j^d	dispersion fraction of the j component [—]
X_j^p	polar fraction of the j component [—]
X_{LS}	adjustable parameter in Φ_G [—]
X_S^p	the polarity of polymer solid [—]

Greek Letters

γ_C	critical surface tension [$mN \cdot m^{-1}$]
γ_c^E	experimental value of critical surface tension [$mN \cdot m^{-1}$]
γ_c^T	theoretical value of critical surface tension [$mN \cdot m^{-1}$]
γ_L	surface tension of liquid [$mN \cdot m^{-1}$]
γ_L^d	the dispersion component of liquid surface tension [$mN \cdot m^{-1}$]
γ_L^h	hydrogen bonding component of liquid surface tension [$mN \cdot m^{-1}$]
γ_L^p	the polar component of liquid surface tension [$mN \cdot m^{-1}$]
γ_S	surface tension of polymer solid [$mN \cdot m^{-1}$]
γ_S^d	the dispersion component of solid surface tension [$mN \cdot m^{-1}$]
γ_S^h	hydrogen bonding component of solid surface tension [$mN \cdot m^{-1}$]
γ_{SL}	the interfacial tension between the solid and the liquid [$mN \cdot m^{-1}$]
γ_S^p	the polar component of solid surface tension [$mN \cdot m^{-1}$]
δ	solubility parameter [—]
δ^p	polarity component of solubility parameter [—]

θ contact angle [deg.]
λ the slope of the Young-Dupré-Good-Girifalco plot [—]
ϕ the intercept of the Young-Dupré-Good-Girifalco plot [—]
Φ_G interaction parameter [—]
Φ_G^o parameter defined in Eq. (9) [—]
Φ_0 indication of polarity in Φ_G [—]
Ψ slope of the log $(1 + \cos\theta)$ vs log γ_L plot [—]

REFERENCES

[1] Ruska, W. S. (1987). *Microelectronic Processing: An Introduction to the Manufacture of Integrated Circuits*, McGraw-Hill: New York, 68–76.
[2] Endo, A., Takada, M., Adachi, K., Takasago, H., Yada, T., & Onishl, Y. (1987). *J. Electrochem. Soc.: Solid-State Sci. Tech.*, *34*, 2522.
[3] Mittal, K. L. (1984). *Polyimides: Synthesis, Characterization, and Applications*, Plenum Press: New York.
[4] Feger, C., Khojasteh, M. M., & Htoo, M. S. (1993). *Advances in Polyimide Science and Technology*, Technomic Publications: Lancaster.
[5] Sroog, C. E. (1979). *J. Polym. Sci.: Macromolecular Reviews*, *11*, 161.
[6] Wilson, A. M. (1984). In: *Use of Polyimides in VLSI Fabrication, in Polyimides,* 1st ed., Mittal, K. L. (Ed.), Plenum Press: New York, 715–733.
[7] Wilson, A. M. (1981). *Thin Solid Films*, *83*, 145.
[8] Sacher, E. & Susko, J. R. (1981). *J. Appl. Polymer Science*, *26*, 679.
[9] Ree, M., Goldberg, M. J., Czornyj, G., Han, H. S., & Gryte, C. C. (1993). *Polym. Mater. Sci. Eng.*, *68*, 126.
[10] Lee, D. H. (1987). *Polymer(korea)*, *11*, 206.
[11] Belluchi, F., Khamis, I., Senturia, S. D., & Lantanison, R. M. (1990). *J. Electrochem. Soc.*, *137*, 1778.
[12] Han, H. S. (1993). Ph.D. Thesis, Columbia University, New York.
[13] Denton, D. D., Day, D. R., Priore, D. F., & Senturia, S. D. (1985). *J. Electronic Materials*, *14*, 119.
[14] Melcher, J., Deben, Y., & Arlt, G. (1989). *IEEE Elecrt. Insul.*, *24*, 31.
[15] Sacherand, E. & Sucko, J. R. (1979). *J. Appl. Polym. Sci.*, *23*, 2355.
[16] Merrem, H. J., Klug, R., & Hartner, H. (1989). In: *New Developments in Photosensitive Polyimid, in Polyimides,* 2nd ed., Mittal, K. L. (Ed.), Plenum Press: New York, 919–931.
[17] Tchangai, E., Segui, Y., & Doukkali, K. (1989). *J. Appl. Polym. Sci.*, *38*, 305.
[18] Jou, J.-H., Huang, R., Huang, P.-T., & Shen, W.-P. (1991). *J. Appl. Polym. Sci.*, *43*, 857.
[19] Kwon, Y. & Kim, K.-H. (2006). *Macromol. Res.*, *14*, 424.
[20] Fox, H. W. & Zisman, W. A. (1950). *J. Colloid Sci.*, *5*, 514.
[21] Johnson, R. E. & Dettre, R. H. (1965). *J. Colloid Sci.*, *20*, 73.
[22] Gaudin, A. M. (1957). *Flotation*, McGraw-Hill: New York, 163.
[23] Adamson, A. W., Shirley, F. P., & Kunichika, K. T. (1970). *J. Colloid Interface Sci.*, *34*, 461.
[24] Fort, T. & Patterson, H. T. (1963). *J. Colloid Sci.*, *18*, 217.
[25] Kitazaki, Y. & Hata, T. J. (1972). *J. Adhes. Soc. Jpn.*, *8*, 131.
[26] Kano, Y. & Akiyama, S. (1992). *Polymer*, *33*, 1690.
[27] Fox, H. W. & Zisman, W. A. (1952a). *J. Colloid Sci.*, *7*, 109.

[28] Fox, H. W. & Zisman, W. A. (1952b). *J. Colloid Sci.*, *7*, 428.
[29] Zisman, A. (1964). In: Treaties on *Contact Angle, Wettability and Adhesion, Advances in Chemistry Series*, American Chemical Society: Washington, DC, No. 43, 1–51.
[30] Fowkes, F. M. (1964). In: Treaties on *Contact Angle, Wettability and Adhesion, Advances in Chemistry Series*, American Chemical Society: Washington, DC, No. 43, 99–111.
[31] Good, R. J. (1964). In: Treaties on *Contact Angle, Wettability and Adhesion, Advances in Chemistry Series*, American Chemical Society: Washington, DC, No. 43, 74–87.
[32] Good, R. J. (1967). In: Treaties on *Adhesion and Adhesive*, Patrick, R. L. (Ed.), Marcel Dekker: New York, Vol. 1, 9–68.
[33] Good, R. J. & Girifalco, L. A. (1960). *J. Phys. Chem.*, *64*, 561.
[34] Kano, Y. & Saito, T. (1988). *Setchaku*, *32*, 396.
[35] Wu, S. (1982a). *Polymer Interface and Adhesion*, Marcel Dekker: New York, 105.
[36] Kaelble, D. H. & Uy, K. C. (1970). *J. Adhes.*, *2*, 51.
[37] Wu, S. (1982b). *Polymer Interface and Adhesion*, Marcel Dekker: New York, 257–259.
[38] Adamson, A. W. (1990a). *Physical Chemistry of Surfaces,* 5th ed., John Wiley & Sons: New York, 389–392.
[39] Ghosh, M. K. & Mittal, K. L. (1996). *Polyimides: Fundamentals and Applications*, Marcel Dekker: New York, 16–18.
[40] Wu, S. (1982c). *Polymer Interface and Adhesion*, Marcel Dekker: New York, 162.
[41] Wu, S. (1982d). *Polymer Interface and Adhesion*, Marcel Dekker: New York, 183.
[42] Adamson, A. W. (1990b). *Physical Chemistry of Surfaces,* 5th ed., John Wiley & Sons: New York, 397–398.
[43] Gutowski, W. (1985). *J. Adhes.*, *19*, 29.
[44] Kim, K.-H. & Kwon, Y. (2005). *J. Chem. Eng. Japan.*, *38*, 641.
[45] Kim, K.-H., Kim, Y.-G., & Kwon, Y. (2007). *Mol. Cryst. Liq. Cryst.*, *470*, 145.
[46] Brandrup, J. & Immergut, E. H. (1989). *Polymer Handbook,* 3rd ed., Wiley-Interscience, John Wiley & Sons: New York, VI/422.